RESEARCH PROGRESS IN MECHANICAL AND MANUFACTURING ENGINEERING
e-ISSN: 2773-4765

RPMME

Vol. 5 No. 1 (2024) 250-258
https://publisher.uthm.edu.my/periodicals/index.php/rpmme

Effects of Various Calcination Times and Temperatures on Zinc Oxide as Gas Sensing for Volatile Organic Compound

Suraini Abdullah[1], Ainun Rahmahwati Ainuddin @ Nordin[1,2*]

[1] *Faculty of Mechanical and Manufacturing Engineering*
Universiti Tun Hussein Onn Malaysia, Parit Raja, Batu Pahat, 86400, MALAYSIA
[2] *Nano Structure and Surface Modification (Nanosurf), Faculty of Mechanical and Manufacturing Engineering*
Universiti Tun Hussein Onn Malaysia, Parit Raja, Batu Pahat, 86400, MALAYSIA

*Corresponding Author: ainun@uthm.edu.my
DOI: https://doi.org/10.30880/rpmme.2024.05.01.029

Article Info

Received: 1 Mac 2024
Accepted: 15 July 2024
Available online: 15 Sept. 2024

Keywords

VOCs, CO, ZnO, XRD, FESEM, EDS

Abstract

The investigation aims to analyse the impact of different calcination temperatures on ZnO nanostructures synthesized via a hydrothermal method. Nine samples, denoted as A_1, A_2, A_3, B_1, B_2, B_3, C_1, C_2, and C_3, were created at temperatures of 400ºC, 500ºC, and 600ºC, each for 0, 2, and 4 hours. Utilizing X-ray Diffraction (XRD), Field-Emission Scanning Electron Microscopy (FESEM), and Energy-Dispersive X-ray Spectroscopy (EDS), the study investigates the structural and morphological changes resulting from various calcination conditions. The analysis confirmed ZnO presence in all samples and presented consistency with the wurtzite ZnO JCPDS card in XRD patterns. FESEM observations indicated a relation between calcination temperature and alterations in ZnO structure morphology, with increased temperatures resulting in reduced thickness and area. The elemental compositions were determined through EDS analysis, indicating the successful synthesis of ZnO in the samples. This research underscores the impact of calcination temperature and time on ZnO nanostructure properties, providing crucial insights for optimizing synthesis parameters and informing applications in fields like photocatalysis, sensors, and biomedical devices. The synthesized ZnO indicates significant potential as a gas sensor material, with substantial effectiveness in detecting volatile organic compounds (VOCs), indicating its usefulness for environmental monitoring and industrial applications.

1. Introduction

In the current era of rapid industrialization, increasing environmental issues, concerns have increased primarily due to hazardous gas releases. Activities such as combustion processes, emissions from wastewater treatment plants, the oil and gas industry, pharmaceutical practices, and natural sources contribute significantly to pollution, threatening human health and the natural ecosystem. [1] Volatile organic compounds (VOCs), identified as organic molecules with specific boiling and vapor pressure parameters, play a pivotal role in atmospheric photochemical reactions, as noted by the United States Environment Protection Agency (EPA). [2] Obviously, VOCs include acetone, ammonia, formaldehyde, methanol, carbon monoxide, and ethanol, each presenting distinct health risks. Specifically, carbon monoxide, being colorless and odorless, poses a serious threat by forming carboxyhemoglobin in the blood, hindering oxygen transport. Ethanol, also colourless and odourless, generated through fermentation, leads to severe health issues. [3] Regulatory bodies must prioritise control measures to address the imperative

need to quantify and minimise VOC emissions. Developing gas sensors, particularly those utilizing metal oxides like zinc oxide (ZnO), stands out as a crucial solution. ZnO's advantageous properties, including robust mechanical strength, chemical stability, wide bandgap, and good conductivity, make it highly suitable for effective gas sensing applications and provide potential for reducing environmental challenges [4]. In this metal oxide producing analysis, the technique that will be implemented in order to successfully construct the synthesized ZnO will be explained in detail. It begins with a hydrothermal process and continues to calcination of the substance at various temperatures. XRD, FESEM and EDS will also be employed to characterize the synthesized ZnO. For instance, the table below provides an illustrative example of previous Field Emission Scanning Electron Microscopy (FESEM) results, providing as a guide to ensure the alignment of the obtained ZnO structure with findings from prior research.

Fig. 1 shows the morphology of the ZnO Array Sample synthesis via hydrothermal methods. Analyzing both figures reveal that sample 1 has a homogeneous one-dimensional needle-like array structure, from which a single needle-like ZnO nanorod has a hexagonal pyramid shape. Also, the sample 2 has a homogeneous delicate three-dimensional (3D) wheatear-like array, in which a wheatear-like ZnO nanostructure consists of numerous kernel-like nanorods orderly attaching on the lateral surfaces of needle-like nanorods to form a hexagonal star pattern observed along a wheatear-like. Furthermore, whether needle-like or kernel-like ZnO nanorods are single crystalline with hexagonal wurtzite structure and space group p63mc [5].

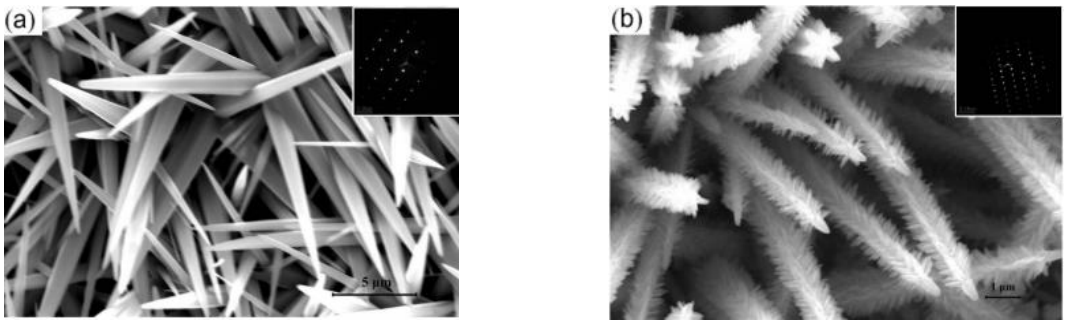

(a) **(b)**

Fig. 1 *SEM Images of 9(a) The Needle-like ZnO Array Sample 1, (b) The Wheatear-like ZnO Array Sample 2 [5]*

Fig. 2 shows the ZnO nanorods synthesis via a simple hydrothermal process for 50 days. Referring to the FESEM image of ZnO nanorods, the synthesized ZnO nanorods had clustered, generating flower-like hierarchical nanostructures [6].

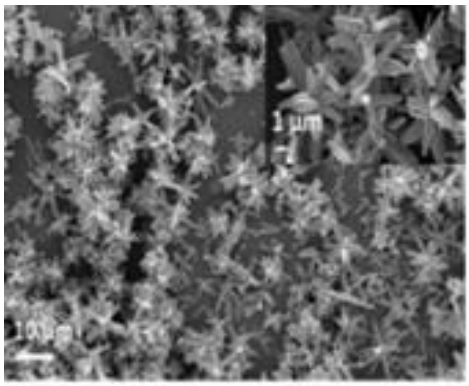

Fig. 2 *The FESEM Image of ZnO Nanorods [6]*

The primary objectives of this study involve synthesizing ZnO nanostructures through a hydrothermal approach, incorporating variations in calcination temperatures and durations. The focus is on developing a gas sensor for detecting volatile organic compounds (VOCs) by employing the hydrothermal synthesis of ZnO structures. The synthesis process utilizes zinc nitrate ($Zn(NO_3)_2$) and ethanol (C_2H_6O) as the growth solution. The subsequent calcination process varies at temperatures of 400, 500, and 600 ºC, with processing times set at 0 hours, 2 hours, and 4 hours. Additionally, the study aims to assess how calcination temperature influences the structural and morphological characteristics of the synthesized ZnO. Various techniques, including X-ray diffraction (XRD) for structural insights, Field Emission Scanning Electron Microscopy (FESEM) for detailed imaging, and Energy Dispersive X-ray Spectroscopy (EDS) for elemental composition analysis, will be employed to comprehensively analyze the morphological characteristics of the synthesized ZnO. Finally, based on the

obtained results, a crucial aspect of the study involves analyzing the gas sensing capabilities of the synthesized ZnO properties for the detection of volatile organic compounds.

2. Methodology

This part will extensively explain the methodology to synthesize ZnO as a gas sensor for VOC detection. It covers ZnO preparation, the hydrothermal method for structure building, XRD, FESEM and EDS characterization.

2.1 General Project Workflow

As indicated in Fig. 3, the details of the process that was implemented throughout this project are shown.

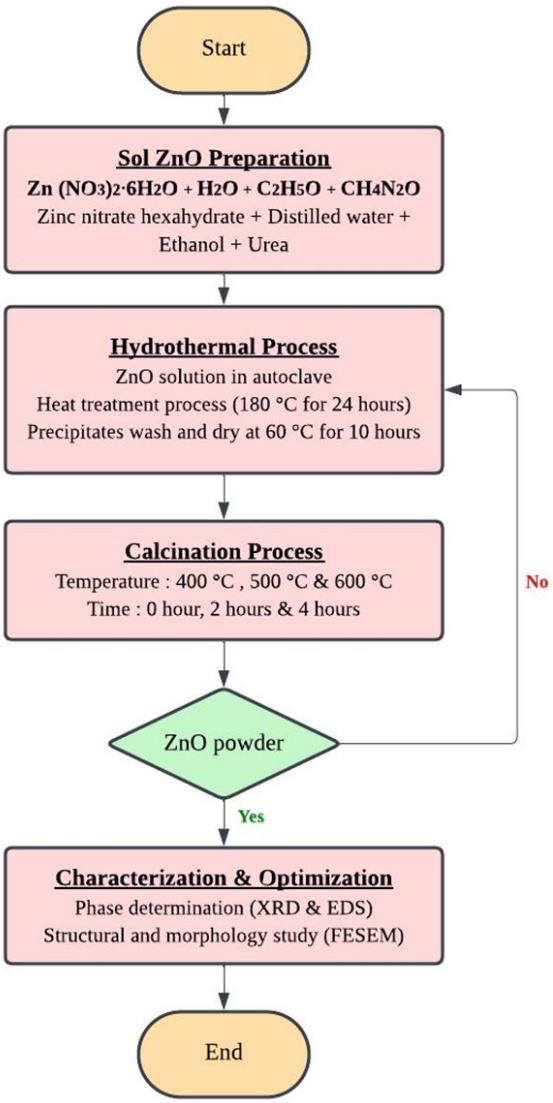

Fig. 3 *General Project Workflow*

2.2 Preparation of Synthesized Zinc Oxide

The hydrothermal process and subsequent calcination are vital for synthesizing ZnO. Zinc nitrate hexahydrate is dissolved in a mix of ethanol and distilled water, and then urea is added. This mixture undergoes hydrothermal growth in a stainless-steel autoclave for 24 hours at 180°C. White precipitates are collected, filtered, washed, dried for 10 hours at 60 °C, and finally subjected to calcination at different temperatures and times, resulting in various samples listed in Table 1.

Table 1 *The List of Sample*

Calcination Time (Hours)	Temperature (ºC)		
	400	500	600
0	A_1	B_1	C_1
2	A_2	B_2	C_2
4	A_3	B_3	C_3

2.3 Characterizations of Synthesized Zinc Oxide

After the ZnO has been synthesized through the hydrothermal method, its structure will be investigated by using XRD, FESEM and EDS.

2.3.1 X-Ray Diffraction (XRD)

XRD is a technique used in materials science to determine a material's atomic and molecular structure. This is accomplished by irradiating a sample of the material with incoming X-rays and then measuring the intensities and scattering angles of the scattered X-rays. [7] The crystal structure and phase transformation were investigated using a Bruker D8 Advance X-ray diffractometer in Germany, employing CuKa radiation within the 20 to 80 2θ degree range. To achieve accurate XRD analysis, obtaining a pure sample and grinding it into a fine powder to reduce additional strain and randomize orientation, aiming for particles smaller than 10 µm or 200 mesh is crucial. The powdered sample should then be evenly smeared onto a glass slide, ensuring a flat upper surface and placed in a sample container. Attention must be given to generating a smooth upper surface and ensuring a random distribution of lattice orientations for an oriented smear. During the XRD process, the intensity of X-rays is recorded as both the sample and detector rotate through their respective angles.

2.3.2 Field Emission Scanning Force Microscopy (FESEM)

FESEM offers topographical and elemental information at magnifications ranging from 10x to 300,000x, with an essentially infinite depth of field. This technique has advantages in evaluating smaller-area contaminations and is compatible with energy dispersive spectroscopy (EDS) at suitable electron-accelerating voltages. It reduces the penetration of low-kinetic-energy electron probes near the material surface and provides high-quality images at low voltages, maintaining the samples' electrical charge. FESEM operates within an accelerating voltage range of 0.5 to 30 kilovolts, eliminating the need for conducting coatings on insulating materials. [8] The process begins by ensuring the samples are conductive for current by applying an extremely thin layer (1.5 - 3.0 nm) of gold or gold palladium, which is carried out in a separate apparatus. Before chemical fastening, materials must undergo rinsing and drying below the critical point to prevent surface tension damage to delicate structures.

2.3.3 Energy Dispersed Spectroscopy (EDS)

Energy-dispersive X-ray spectroscopy (EDS), also known as EDX or XEDS, is an analytical method used to determine a sample's elemental or chemical composition. It enables the identification of elemental constituents at specific locations and the creation of elemental distribution maps across an imaged area. [9] The purpose of EDS is to determine the content of zinc oxide in the samples. It is critical to begin SEM because it is essential for EDS testing. The proper positioning and preparation of samples are crucial for accurate analysis. Using carbon adhesive tape, affix the samples onto the specimen holder, ensuring they remain flat. Next, place the specimen in the SEM/EDS chamber, arranging them in a circular configuration to optimize space. Transfer the SEM results to the EDS display system for further analysis before evaluating the final results.

3. Analysis and Discussion

3.1 Introduction

This chapter focuses on analysing results obtained from characterizing and optimizing ZnO nanostructures using techniques such as XRD, FESEM, and EDS. Using these methods, it aims to evaluate various aspects, including crystallinity, phase, surface morphology, and elemental analysis. Detailed discussions are essential to meet the project objectives. The characteristics of ZnO powder synthesized via hydrothermal and calcination methods will be scrutinized based on the achieved results, which involve nine different samples prepared at varying temperatures. This section will examine ZnO formation test outcomes from XRD, FESEM, and EDS machines, aligning with the research scopes to discuss crystallography obtained from XRD, morphologies from FESEM and element content via EDS.

3.2 X-Ray Diffraction (XRD)

XRD was used to analyse the structural aspects of substrate samples grown under various factors like precursor, time, and temperature post-hydrothermal and calcination processes. Variations were observed in Fig. 4 due to distinct calcination temperatures and durations for each sample. Each figure presents detailed analyses with three diffractograms depicting ZnO products after calcination at 400°C, 500°C, and 600°C. These diffractograms display XRD patterns for calcination durations of 0 hours, 2 hours, and 4 hours, within the 2θ range of 20^0 to 80^0 corresponding to wurtzite ZnO (JCPDS card No. 36-1451).

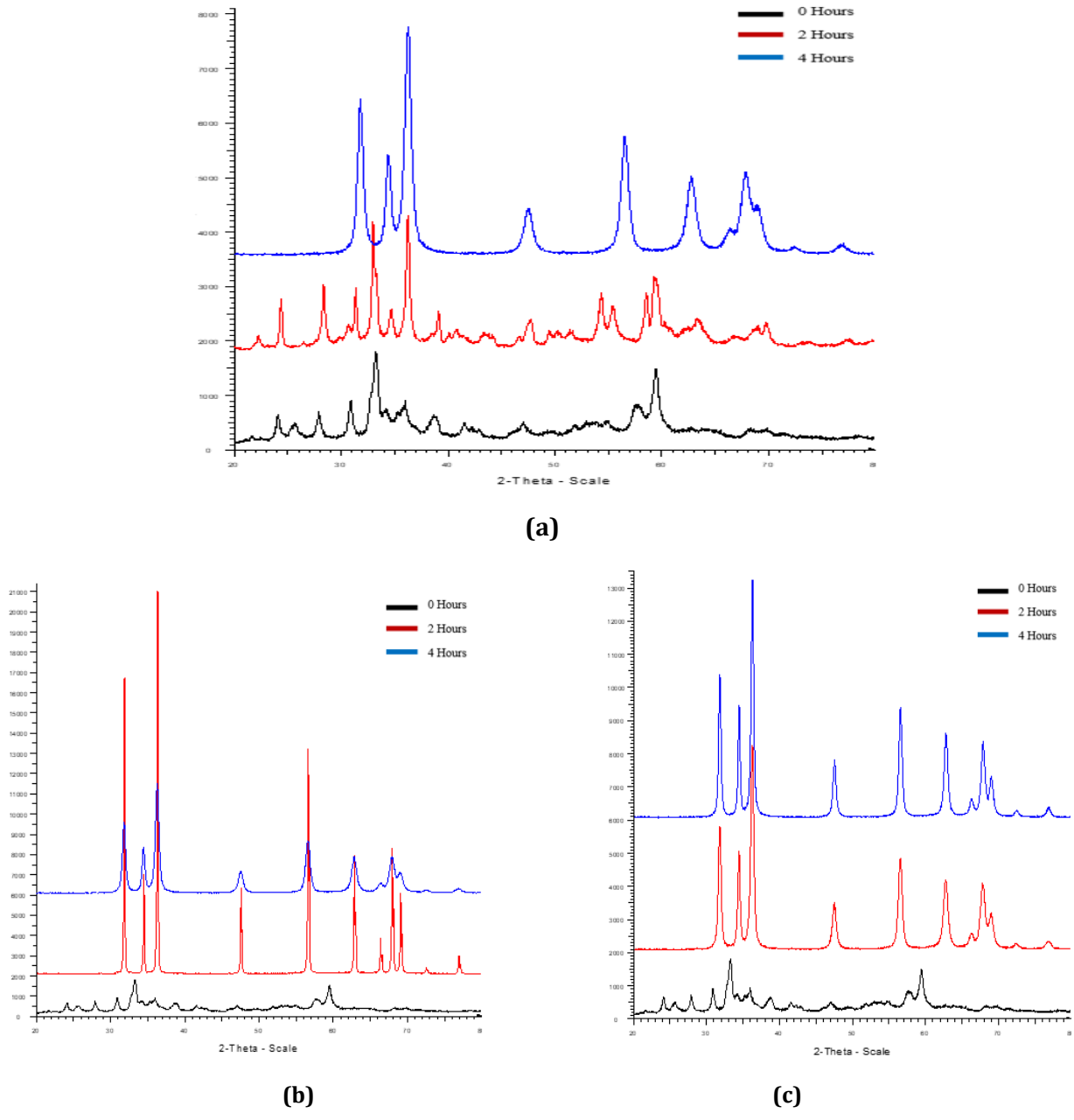

Fig. 4 *The XRD Pattern of ZnO Obtained (a) sample A_1, A_2 and A_3 ; (b) sample B_1, B_2 and B_3 ; (c) sample C_1, C_2 and C_3*

The XRD patterns of samples A_1, B_1, and C_1 show broad peaks, suggesting smaller particle sizes or less crystalline ZnO due to a shorter calcination time, which is 0 hours, indicating incomplete crystallization. Sample A_2 displays a slightly broad peak, possibly indicating the presence of crystalline material that does not align with the expected XRD pattern. Besides, sample B_2 closely matches the JCPDS pattern but shows considerable differences in peak heights. In contrast, samples A_3, B_3, C_2, and C_3 exhibit XRD peaks highly similar to JCPDS card No. 36-1451, confirming a match with the wurtzite structure of ZnO. This similarity indicates these samples were appropriately calcined, forming the predicted crystalline structure for gas sensing. These findings align with the referenced research, emphasizing increased crystallinity at higher calcination temperatures, leading to improved accuracy

and peak intensities. The most distinct (101) plane peak signifies the presence of pure crystalline ZnO, supporting the conclusion that higher-temperature calcination enhances crystallinity. [10]

3.3 Field Emission Scanning Electron Microscopy (FESEM)

Samples subjected to hydrothermal processing were analyzed to identify surface characteristics. Fig. 5 illustrates the morphology of ZnO nanostructures observed through SEM and FESEM resulting from hydrothermal synthesis at temperatures of 400°C, 500°C, and 600°C for 0 hours.

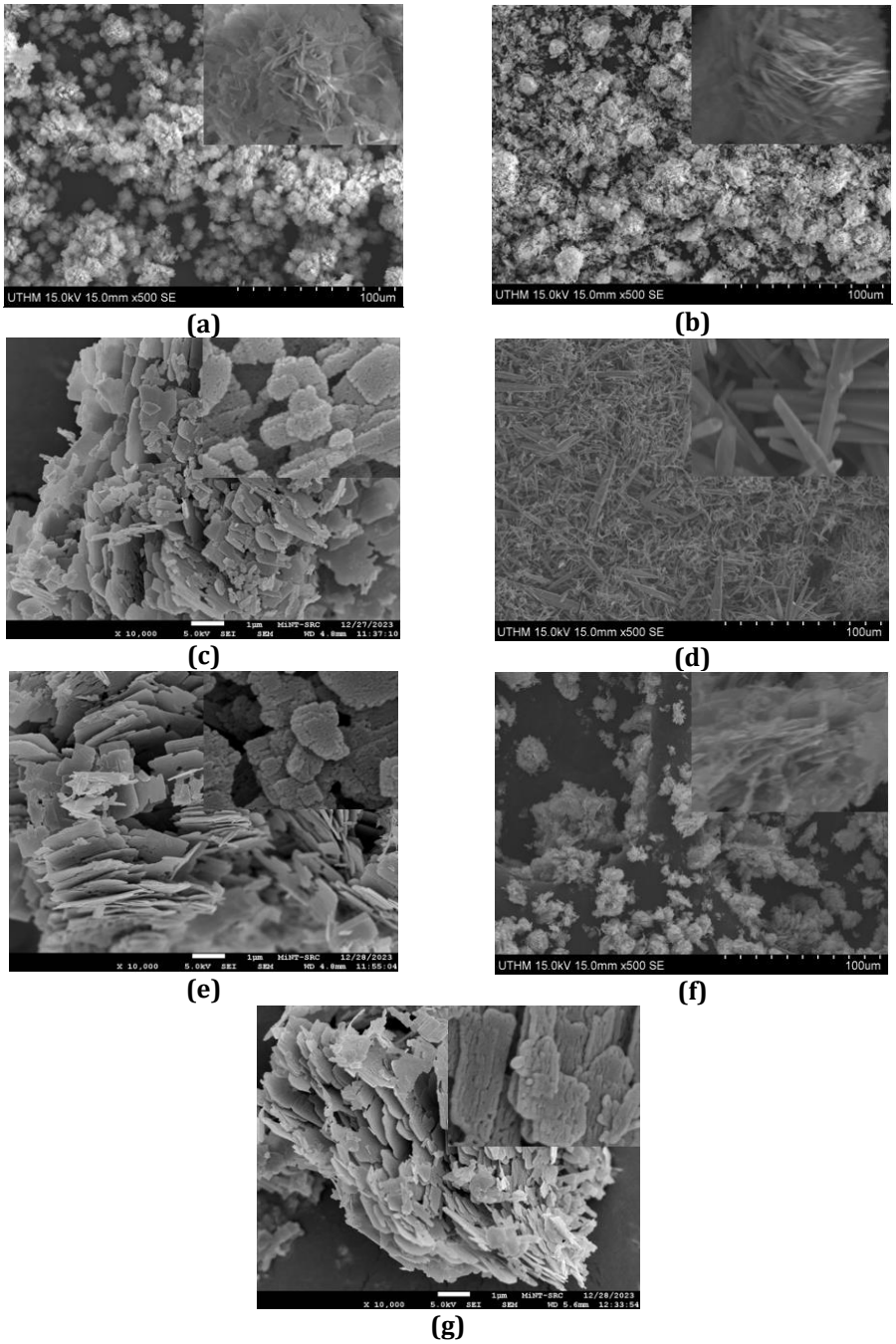

Fig. 5 *The ZnO Morphology Examined via SEM and FESEM (a) Sample A_1, B_1, C_1; (b) Sample A_2; (c) Sample A_3; (d) Sample B_2; (e) Sample B_3; (f) Sample C_2; (g) Sample C_3*

Additionally, ImageJ software was utilized to determine the particle size of ZnO structures observed via FESEM, specifically for samples A_3, B_3, and C_3. This software facilitated the measurement of particle size by calculating the structure thickness. In sample A_3, the identified thickness is 48.275 µm. Besides, sample B_3 shows a thickness of 45.491 µm. Meanwhile, sample C_3 exhibits thickness values of 41.045 µm. An inverse relationship between calcination temperature and mean area or length indicates that higher temperatures lead to thinner structures. For instance, C_3 exhibited a thinner structure compared to A_3 and B_3. This correlation implies that, in

line with prior research, a thin and evenly surfaced structure, achievable through modern manufacturing technologies, is conducive to an effective sensing layer application [11].

Regarding the distribution of mean pore areas across the surface structure, sample A_3 displayed an average pore area of 1578.57 μm^2, while sample B_3 had a significantly smaller mean pore area of 2472 μm^2. Sample C_3 exhibited an even smaller mean pore diameter of 2764 μm^2. The porous structure in these ZnO samples aligns with prior research, providing numerous surface-active sites that enhance gas-sensing reactions. This configuration reduces gas diffusion resistance, especially for VOCs, resulting in exceptional gas-sensing properties. The large contact surface area facilitates gas molecule adsorption and effective diffusion, contributing to significant gas response, rapid response, and recovery times in VOCs detection [12].

When examining crystallite sizes within the ZnO structure, sample A_3 showed a mean area of 44914.7 μm^2, sample B_3 exhibited a slightly larger mean area of 59074.7 μm^2, and sample C_3 demonstrated a considerably larger mean area of 111289 μm^2. As previously stated, the XRD peaks of samples A_3, B_3, C_2, and C_3 correspond to the ones on JCPDS card No. 36-1451. This similarity suggests that the samples experienced appropriate calcination in terms of duration and temperature, resulting in the expected crystalline structure. The alignment of the expected crystalline structure in all of these samples is consistent with findings from a referenced article, in which increasing temperature was found to improve crystallinity, even with the result of increased crystalline size and reduced surface area [10].

3.4 Energy Dispersed Spectroscopy (EDS)

The resulting EDS graph (Fig. 6) displayed peaks representing the elemental content of the samples, primarily zinc and oxygen, expected in ZnO particles, providing the most mass. A successful synthesis of ZnO was determined when zinc and oxygen are the primary elements that provide the most mass, as expected when ZnO particles form.

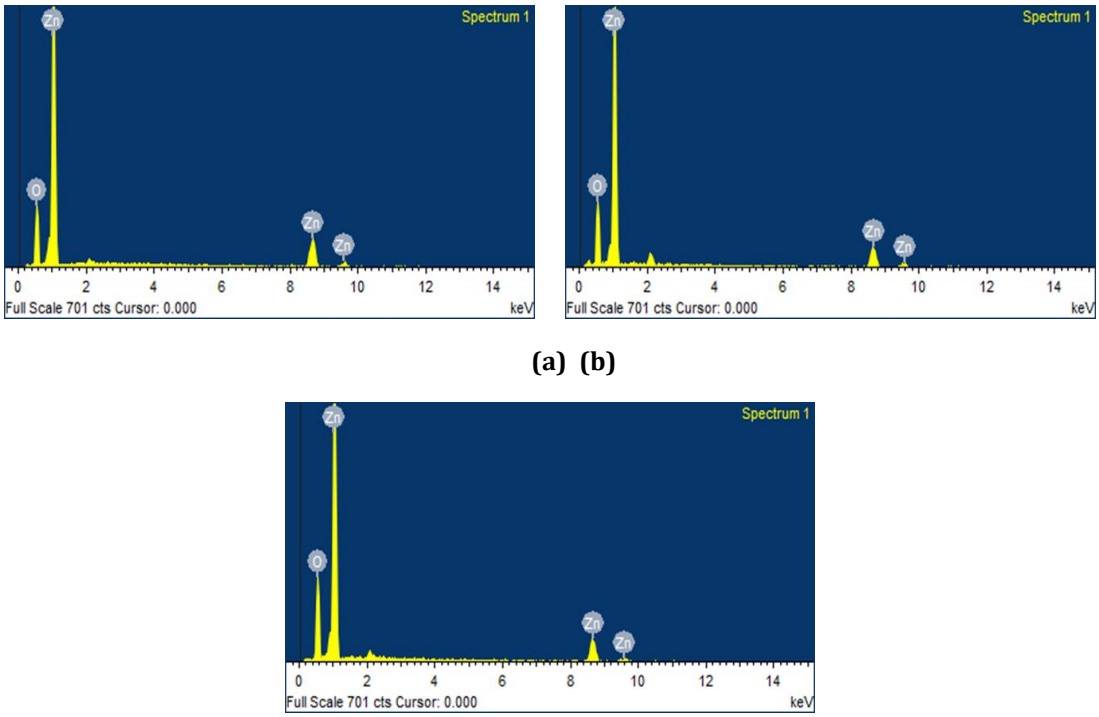

Fig. 6 *The EDS Graph of ZnO (a) Sample A_3; (b) Sample B_3; (c) Sample C_3*

Table 2 *Data Base on ZnO for Sample A_3*

Element	Peak Omitted (keV)	%Weight	%Atomic
Zn	2.075	79.87	49.27
O	-	20.13	50.73
Total		100	100

Following the data from the ZnO database at 4 hours for 400°C shown in Table 2, the analysis indicates a zinc weight percentage of 79.87% with its peak observed at 2.075 keV. Despite that, oxygen constitutes only 20.13% of weight. In terms of atomic percentages, zinc accounts for 49.27%, while oxygen consists of the remaining 50.73%.

Table 3 *Data Base on ZnO for Sample B_3*

Element	Peak Omitted (keV)	%Weight	%Atomic
Zn	2.055	74.59	41.81
O	0.265	25.41	58.19
Total		100	100

Afterwards, in the ZnO database at 4 hours and 500°C (Table 3), it can be recognised that the zinc weight percentage of 74.59%, indicated by peaks omitted at 2.055 keV. In contrast, oxygen constitutes only 25.41% by weight, observed with peaks omitted at 0.265 keV. Additionally, regarding atomic percentages, zinc forms 41.81% of the total, while oxygen contributes 58.19%. It is significant to note that zinc has the largest peaks of any elemental component.

Table 4 *Data Base on ZnO for Sample C_3*

Element	Peak Omitted (keV)	%Weight	%Atomic
Zn	2.055	77.49	45.73
O	-	22.51	54.27
Total		100	100

Finally, at 4 hours and 600°C (Table 4), the analysis in the ZnO database indicated a zinc weight percentage of 77.49%, with the peak recorded at 2.055 keV. In comparison, oxygen forms only 22.51% of the total weight. Furthermore, in terms of atomic percentages, zinc contributes 45.73%, whereas oxygen accounts for 54.27%.

4. Conclusion

In conclusion, this study successfully examined synthesised ZnO nanostructures using a hydrothermal method with varied calcination temperatures and durations. Nine samples, which are denoted as A1, A2, A3, B1, B2, B3, C1, C2, and C3, were synthesised at 400ºC, 500ºC, and 600ºC for intervals of 0 hours, 2 hours, and 4 hours. Comprehensive analysis using XRD, FESEM, and EDS revealed crucial insights. XRD analysis confirmed the presence of ZnO in all samples, with broad peaks indicating smaller particle sizes due to insufficient calcination time and sharp peaks suggesting appropriate calcination times and increased crystallite sizes. FESEM observations showed a decrease in structure thickness with higher calcination temperatures. EDS revealed successful ZnO synthesis when ZnO elements are present in the samples. This study extensively explores the potential of synthesised ZnO as a gas sensor for detecting volatile organic compounds (VOCs). XRD analysis of samples A_3, B_3, C_2, and C_3 confirms their alignment with the specific wurtzite structure of ZnO, indicating suitable calcination conditions for gas sensing. Particle size measurements using ImageJ and FESEM results for A_3, B_3, and C_3 demonstrate an inverse relationship between structure thickness and gas-sensing performance, emphasising the effectiveness of thin, even surfaces for functional sensing layers. [11] Additionally, the study highlights variations in mean pore areas, with A_3 exhibiting a larger pore area than B_3 and C_3. This porous structure enhances gas-sensing properties, particularly for VOCs, evidenced by significant gas response and rapid recovery times.

Acknowledgement

The authors would like to thank the Faculty of Mechanical and Manufacturing Engineering, Universiti Tun Hussein Onn Malaysia, for supporting the research.

Conflict of Interest

The authors declare that there is no conflict of interest regarding the publication of the paper.

References

[1] M. Taheripour, N. Yasrebi, S. Nasresfahani, and M. H. Sheikhi, “Highly sensitive and fast-response volatile organic compounds sensors based on star-shaped BaTiO3/ZnO heterostructures,” IEEE Sens J, vol. 21, no. 4, pp. 4225–4232, Feb. 2021, doi: 10.1109/JSEN.2020.3033210.

[2] Carpenter, P. C., Ciccioli, P., Goldstein, A., Hamilton, J. F., Hoffmann, T., Lewis, A. C., & Williams, J. (2007). Volatile organic compounds in the atmosphere. Oxford, Blackwell.
[3] A. Sarkar, M. Chanda, IEEE Electron Devices Society. Kolkata Chapter, and Institute of Electrical and Electronics Engineers, Proceedings of International conference on 2018 IEEE Electron Device Kolkata Conference (EDKCON): 24-25 November, 2018, Kolkata, West Bengal, India : place: The Pride Hotel, Kolkata.
[4] J. R. F. Foronda, L. G. Aryaswara, G. N. C. Santos, S. N. V. Raghu, and M. A. Muflikhun, "Broad-class volatile organic compounds (VOCs) detection via polyaniline/zinc oxide (PANI/ZnO) composite materials as gas sensor application," Heliyon, vol. 9, no. 2, Feb. 2023, doi: 10.1016/j.heliyon.2023.e13544.
[5] Zhang, Z., Yan, J., You, T., Li, J., & Tian, J. (2012, August). Hydrothermal fabrication and optical properties of wheatear-like ZnO array. In 2012 12th IEEE International Conference on Nanotechnology (IEEE-NANO) (pp. 1-5). IEEE. https://doi.org/ 10.1109/NANO.2012.6322106
[6] M. Taheripour, N. Yasrebi, S. Nasresfahani, and M. H. Sheikhi, "Highly sensitive and fast-response volatile organic compounds sensors based on star-shaped BaTiO3/ZnO heterostructures," IEEE Sens J, vol. 21, no. 4, pp. 4225–4232, Feb. 2021, doi: 10.1109/JSEN.2020.3033210.
[7] "D8 ADVANCE | Bruker." Accessed: Jul. 02, 2023. [Online]. Available: https://www.bruker.com/en/products-and-solutions/diffractometers-and-x-ray-microscopes/x-ray-diffractometers/d8-advance-family/d8-advance.html
[8] "Field Emission Scanning Electron Microscopy (FESEM) – PhotoMetrics." Accessed: Jun. 27, 2023. [Online]. Available: https://photometrics.net/field-emission-scanning-electron-microscopy-fesem/
[9] A. F. Ismail, K. C. Khulbe, and T. Matsuura, "RO Membrane Characterization," in Reverse Osmosis, Elsevier, 2019, pp. 57–90. doi: 10.1016/b978-0-12-811468-1.00003-7.
[10] S. C. Patil et al., "Calcination temperatures influence the chemo-resistive gas sensing properties of biogenic zinc oxide nanoparticles with antibacterial activity," Inorg Chem Commun, vol. 153, Jul. 2023, doi: 10.1016/j.inoche.2023.110847.
[11] S. Ma, L. Shen, S. Ma, J. Wen, and J. Xu, "Emerging zinc stannate and its application in volatile organic compounds sensing," Coordination Chemistry Reviews, vol. 490. Elsevier B.V., Sep. 01, 2023. doi: 10.1016/j.ccr.2023.215217.
[12] A. Tanneeru et al., "National Science Foundation (NSF) Award Number EEC-1160483."